Efficient Conversion of Thermal Energy into Hydrogen: Comparing Two Methods to Reduce Exergy Losses in a Sulfuric Acid Decomposition Reactor

ARTICLE *in* INDUSTRIAL & ENGINEERING CHEMISTRY RESEARCH · SEPTEMBER 2009

Impact Factor: 2.59 · DOI: 10.1021/ie801585e

4 AUTHORS:

Leen Volkert van der Ham
TNO
21 PUBLICATIONS **137** CITATIONS
SEE PROFILE

Joachim Gross
Universität Stuttgart
90 PUBLICATIONS **2,890** CITATIONS
SEE PROFILE

A.H.M. Verkooijen
Delft University of Technology
101 PUBLICATIONS **799** CITATIONS
SEE PROFILE

Signe Kjelstrup
Norwegian University of Science and Tech…
316 PUBLICATIONS **3,721** CITATIONS
SEE PROFILE

PROCESS DESIGN AND CONTROL

Efficient Conversion of Thermal Energy into Hydrogen: Comparing Two Methods to Reduce Exergy Losses in a Sulfuric Acid Decomposition Reactor

Leen V. van der Ham,[†] Joachim Gross,*[,†] Ad Verkooijen,[†] and Signe Kjelstrup[†,‡]

Department of Process & Energy, Delft University of Technology, Delft, The Netherlands, Department of Chemistry, Norwegian University of Science and Technology, Trondheim, Norway

Two methods for increasing the exergy efficiency of thermochemical processes for the production of hydrogen from water and high temperature thermal energy are presented and compared. Increasing the exergy efficiency is equivalent to reducing the entropy production. Starting from a reference reactor for the decomposition of sulfuric acid, two new reactor designs are developed that both reduce the entropy production by 26%. The first design uses optimal control theory to obtain a more uniform distribution of the entropy production. As a result of this functional optimization we obtain optimal temperature profiles over the reactor length. This optimized design is found to perform the best, but it requires significant changes in the heating equipment in order to approximately realize the optimal temperature profiles. A second design is obtained by increasing the reactor length. This leads to a higher pressure drop and requires additional compressor duty.

1. Introduction

Driven by the need for affordable, environmentally friendly, and reliable energy sources and carriers, the development of thermochemical processes for the production of hydrogen from water has received considerable attention.[1] High temperature thermal energy is used as energy source, originating from nuclear reactors or solar collectors. Naturally, a high efficiency is essential for the feasibility of such processes.

1.1. Energy and Exergy Efficiencies. The performance of energy conversion processes can be evaluated using several types of efficiencies.[2] Nowadays, the most commonly used efficiency is based on the first law of thermodynamics. It is called the energy efficiency and is defined as the useful energy output divided by the total energy input. In the case of hydrogen production from thermal energy, this reduces to the ratio between the chemical energy stored in the produced hydrogen and the amount of thermal energy that is added to the process.

The energy efficiency is based on quantities of energy, but it says nothing about the quality of the energy that is used. The quality of energy is usually described by its potential to perform work, also known as exergy. The difference between the exergy inputs and outputs of a process is the amount of work that has been consumed or produced. For each work consuming process, there exists a minimum amount of required work, which is called the ideal work. In practice the amount of consumed work is always larger than the ideal work because of irreversibilities that are present in the process, as given by the second law of thermodynamics, and the difference between these two amounts is called the lost work. The exergy efficiency of a work consuming process is defined as the ratio between the ideal work and the actual amount of consumed work. In the case of hydrogen production from thermal energy, the exergy efficiency is equal to the ratio between the exergy of the produced hydrogen and the exergy of the thermal energy that is added to the process.

* To whom correspondence should be addressed. E-mail: j.gross@tudelft.nl. Tel.: +31-152786734. Fax: +31-152782460.
[†] Delft University of Technology.
[‡] Norwegian University of Science and Technology.

Nowadays, it is increasingly argued that it is more important to optimize the exergy efficiency than the energy efficiency. Contrary to the energy efficiency, the exergy efficiency always gives meaningful and useful values. In addition, it can be used to indicate possible improvements. More details and examples on optimizing exergy efficiency or exergy analysis are discussed for example by Kotas,[3] Leites et al.,[4] Rosen and Scott,[5] and Bejan et al.[6] In the case of hydrogen production from thermal energy, optimization of the exergy efficiency can be translated into minimizing the average temperature at which the thermal energy is added or reducing heat emissions to the environment. In general, optimization of the exergy efficiency is equal to minimization of the lost work, which is equivalent to minimization of the entropy production according to the Gouy−Stodola theorem.[7]

1.2. Minimizing Entropy Production in Practice. From a thermodynamical viewpoint it is always useful to minimize entropy production, but the actual industrial process and equipment design is driven by costs rather than by thermodynamic variables. By including economical evaluations in the optimization, however, the results become dependent on the current socio-political situation and on varying technical maturity in different fields. The entropy production is by itself unambiguous and independent of time. This is why we deliberately chose to perform a purely thermodynamic optimization in this study. It is of course interesting to perform an analysis that includes economics, for example using an exergo-economics approach.[6] The economic trade-off is between lower operational costs, caused by a higher efficiency and indicated by lower entropy production, and higher investment costs, caused by the need for more complex equipment.

1.3. Approaches to Reduce Entropy Production. When identifying approaches to reduce the entropy production of a process unit, it is necessary to consider its design. The first step in the design of a process unit is typically to define its primary objective, for example the transfer of a certain amount of heat, the realization of a certain displacement, or the conversion of a certain amount of chemicals. The next step is to define the time

10.1021/ie801585e CCC: $40.75
Published on Web 08/06/2009

frame in which this objective has to be achieved, which is closely related to the size of the unit. Both the primary objective and the time frame can give additional secondary objectives. The combination of the process unit objectives and the time frame defines the average rates of change that are required. According to the theory of irreversible thermodynamics these rates, also called fluxes, are linear combinations of their driving forces, using coupling coefficients as proportionality factors. And the total entropy production is given by the product sum of the conjugate fluxes and forces.[7]

In a plug-flow reactor model there are three phenomena that produce entropy: heat transfer, frictional flow, and chemical reactions.[7] The three corresponding fluxes are not coupled, so each flux is the product of a single driving force and transport coefficient only. In this case the total entropy production is simply the sum of the squared fluxes (J_i) divided by their transport coefficients (L_{ii}). The entropy production of each single flux−force pair (σ_i) is then given by

$$\sigma_i = \frac{J_i^2}{L_{ii}} \tag{1}$$

If the entropy production is distributed evenly over the reactor, we speak of equipartition of entropy production. This means that exactly the same amount of entropy is produced at every point in the reactor. It can be reasoned that for a given objective, a constant transport coefficient, and a given time frame (or space), equipartition of entropy production minimizes the entropy production. This becomes plausible when considering an ideal even distribution of a single flux. Starting from this even distribution, any local decrease of the flux needs to be countered by an increase of the flux elsewhere in the process unit, in order to maintain the defined average flux. Because the entropy production is proportional to the squared flux, the decrease in entropy production due to the local decrease of the flux is always smaller than the increase in entropy production due to the corresponding increase of the flux. So any deviation from an even distribution of the flux always increases the entropy production. It can therefore be concluded that the optimal distribution of the flux is an even distribution. This also implies that the driving force and the entropy production of this flux should have an even distribution. And given that the fluxes are uncoupled, the total entropy production should also have an even distribution. Equipartition of entropy production and the equipartition of forces were discussed in more detail by Tondeur and Kvaalen[8] and by Kjelstrup, Sauar, and co-workers.[9,10]

With a predefined primary objective and all the preceding in mind, we can identify three theoretical approaches to reduce the entropy production. The first approach is to increase the time frame, for example, by increasing the reactor length. This results in lower average fluxes and thus less entropy production. The second approach is to ensure a distribution of the entropy production as even as possible. The last approach is to increase the value of the transport coefficients, for example, by improving catalyst properties, which also results in less entropy production. Looking at eq 1, we see that changes in the time frame affect the entropy production to a larger extent than the changes in the transport coefficients.

1.4. Main Objective. The three theoretical approaches can be pursued using different practical procedures, which involve different changes in the design of the process unit. The aim of this study is to compare a method based on the first approach with a method based on the second approach, by applying both methods to a plug-flow reactor for the decomposition of sulfuric acid.

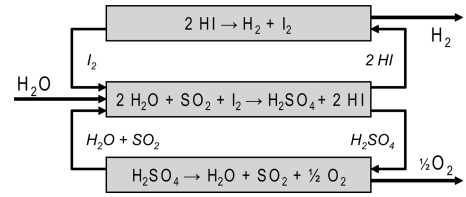

Figure 1. Schematic of the sulfur−iodine process for the production of hydrogen from water.[1]

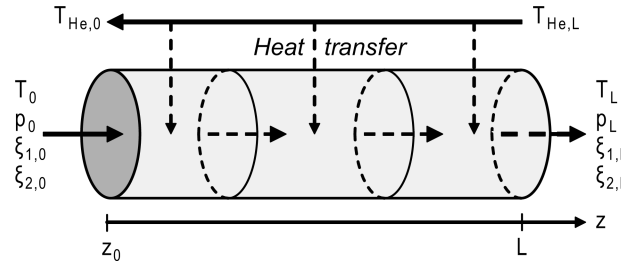

Figure 2. Schematic of the plug-flow reactor configuration.

The first method we use to reduce the entropy production increases the reactor length, since that increases the residence time; it will be referred to as the elongation method. In the second method we follow the work of Johannessen and Kjelstrup.[11] They applied optimal control theory for the first time to minimize the entropy production in a plug-flow reactor, yielding results that were characterized by equipartition of entropy production. This method will be referred to as the optimization method.

2. The Sulfuric Acid Decomposition Reactor

Sulfuric acid decomposition is an essential step in several thermochemical processes for the production of hydrogen from water, using high temperature thermal energy as energy source.[1] An example of such a process is shown in Figure 1.

The gas phase sulfuric acid decomposition reaction can be split into two endothermic subreactions. The first subreaction is the dissociation of sulfuric acid into sulfur trioxide and water I; the second one is the decomposition of sulfur trioxide into sulfur dioxide and oxygen II.

$$H_2SO_4 \rightarrow SO_3 + H_2O \tag{I}$$

$$SO_3 \rightarrow SO_2 + \frac{1}{2}O_2 \tag{II}$$

Dissociation occurs spontaneously at temperatures typically above 350 °C. Decomposition is a catalyzed reaction starting at temperatures between 750 and 900 °C.[12] A standard reactor that can be used for these reactions is a tubular packed bed reactor. Another option that is discussed by Brown et al. is a printed circuit heat exchanger.[13] The modeling and optimization of both options are quite similar. We use a tubular packed bed reactor in our study.

2.1. The Reactor Model. A one-dimensional plug-flow reactor model is assumed. Further we assume that the chemical reactions are kinetically limited, so no internal or external mass or heat transfer limitations exist. Some of these assumptions are quite strong, but their effect on the results will be very small because we are comparing reactors cases that all use the same assumptions. The reactor is schematically illustrated in Figure 2.

The system consists of a tubular reactor with diameter D and length L, which is taken along the length-coordinate z. The reactor is filled with spherical catalyst particles of diameter D_p. The loading of catalyst particles is given by bed density ρ_b, which is the mass of catalyst per reactor volume. The void fraction of the catalyst bed is given by ε. The variables that are used to describe the state of the gaseous reaction mixture are the pressure p, the temperature T, and the extents of reaction ξ_j of the two chemical reactions I and II. The reactor is surrounded by counter-currently flowing helium that serves as heating utility. Its temperature profile along the reactor length is given by $T_{He}(z)$.

2.2. Conservation Equations. For each of the four state variables a conservation equation is used to describe their change along the reactor length. The change in pressure is described by Ergun's equation, which is derived from the momentum balance

$$\frac{dp}{dz} = -\left(\frac{150\eta}{D_p^2}\frac{(1-\varepsilon)^2}{\varepsilon^3} + \frac{1.75\rho_0 v_0}{D_p}\frac{1-\varepsilon}{\varepsilon^3}\right)v \tag{2}$$

In this equation η is the viscosity of the gas, ρ_0 is the gas density at the reactor inlet, v is the gas velocity, and v_0 is the gas velocity at the reactor inlet. The ideal gas law is used to calculate the gas velocity. For the change in temperature an energy balance is used

$$\frac{dT}{dz} = \frac{\pi D J'_q + A_c\rho_b\sum_j (r_{m,j}(-\Delta_r H_j))}{\sum_i (F_i C_{p,i})} \tag{3}$$

where J'_q is the measurable heat flux through the reactor wall, A_c is the cross sectional area of the reactor, r_m is the reaction rate per catalyst weight, $\Delta_r H$ is the enthalpy of reaction, F_i is molar flow rate, and $C_{p,i}$ is the heat capacity of the components. The mole balances describe the change in extents of reaction, they are both defined with respect to sulfur trioxide and using the initial molar flow rate of sulfur trioxide $F_{SO_3,0}$

$$\frac{d\xi_j}{dz} = \frac{A_c\rho_b}{F_{SO_3,0}} r_{m,j} \tag{4}$$

Some of the reactor designs that are discussed use a constant helium flow rate. In this case the energy balance can be used to describe the change in helium temperature:

$$\frac{dT_{He}}{dz} = \frac{\pi D J'_q}{F_{He} C_{p,He}} \tag{5}$$

The measurable heat flux that is used in eqs 3 and 5 is given by

$$J'_q = UT^2\left(\frac{1}{T} - \frac{1}{T_{He}}\right) \approx UT_{He}T\left(\frac{1}{T} - \frac{1}{T_{He}}\right) = U(T_{He} - T) \tag{6}$$

Where U is the overall heat transfer coefficient. The expressions at both sides of the almost equal sign give very comparable results. The expression at the left-hand side of the almost equal sign is used in the model because it proved to simplify the numerical solution methods.

2.3. Entropy Production. The one-dimensional local entropy production (σ) in a plug-flow reactor is given by irreversible thermodynamics as

$$\sigma = \pi D J'_q\left(\frac{1}{T} - \frac{1}{T_{He}}\right) + A_c v\left(-\frac{1}{T}\left(\frac{dp}{dz}\right)\right) + A_c\rho_b\sum_j r_{m,j}\left(-\frac{\Delta_r G_j}{T}\right) \tag{7}$$

The first term on the right-hand side is the flux−force pair for heat transfer, the second term is the flux−force pair for frictional flow, and third term represents the flux−force pairs for the chemical reactions.[7] Here, $\Delta_r G$ is the Gibbs energy of reaction. The total entropy production dS_{irr}/dt is then given by the integral over the entire reactor length, starting from its inlet z_0 to its outlet L

$$\frac{dS_{irr}}{dt} = \int_{z_0}^{L} (\sigma)\, dz \tag{8}$$

2.4. Reaction Rates. According to irreversible thermodynamics, each of the fluxes should be a function of the driving forces. It is therefore essential that a reversible rate expression is used when modeling the reaction rate and not an irreversible rate expression. Because no detailed information on the reaction mechanism and corresponding reaction orders could be found for both subreactions, all components are assumed to have a stoichiometric reaction order. These rate expressions are used

$$r_1 = k_1\left(p_{H_2SO_4} - \frac{p_{H_2O}p_{SO_3}}{K_1}\right) \tag{9}$$

$$r_2 = k_2\left(p_{SO_3} - \frac{p_{SO_2}\sqrt{p_{O_2}}}{K_2}\right) \tag{10}$$

where k_i is the rate constant, p_i is the partial pressure, and K_i is the equilibrium constant. These rate expressions result in nonlinear flux−force relations for the chemical reactions. It is discussed by de Groot and Mazur that irreversible thermodynamics can still be used to describe chemical reactions in this special case.[14] More information on the values of the rate constants that are used is presented in the Supporting Information.

3. Minimization of Entropy Production Using Optimal Control Theory

One of the approaches to reduce entropy production is to try and obtain an even distribution. In practice it is often impossible to obtain a perfectly even distribution because of constraints on the system. Johannessen and Kjelstrup developed a constrained optimization scheme based on optimal control theory that minimizes the entropy production in a plug-flow reactor, using the temperature profile of the heating or cooling utility and the reactor length as optimization variables.[11] Their optimization results are characterized by subsection(s) with constant thermodynamic forces and local entropy production. This illustrates that this optimization scheme is useful in approaching an even distribution as much as possible.

3.1. The Optimization Problem. The aim of the optimization is to find the profile of the heating utility ($T_{He}(z)$) that minimizes the total entropy production in the plug-flow reactor, while obeying a number of constraints. The first four optimization constraints are of course the conservation eqs 2−4, where eq 4 is used twice for the two reactions. They constrain the change in the state variables along the reactor. The next eight constraints concern the values of the four state variables at the reactor inlet and outlet. They are constrained in order to keep full compatibility with the rest of the process. This ensures for example that the same amount of chemicals is converted in the

systems to be compared, which is the primary objective of the decomposition reactor.

3.2. Optimal Control Theory. The optimization scheme is based on optimal control theory. This theory provides a set of necessary conditions that need to be satisfied in order to attain a minimum. First the Hamiltonian H is introduced as

$$H(x_n(z), \lambda_n(z), T_{He}(z)) = \sigma(x_n(z), T_{He}(z)) + \sum_{i=1}^{n} \lambda_i f_i(x_n(z), T_{He}(z)) \quad (11)$$

Here, x_n represent the four state variables p, T, ξ_1, and ξ_2; λ_n are four corresponding multiplier functions and f_n are eqs 2−4 that constrain the changes in the state variables, where the index $n \in \{1,..., 4\}$, because eq 4 is used twice. The helium temperature profile ($T_{He}(z)$) is the control variable. The nine necessary conditions related to the reactor profiles are then given by

$$\frac{dx_n}{dz} = f_n \quad (12)$$

$$\frac{d\lambda_n}{dz} = -\frac{\partial H}{\partial x_n} \quad (13)$$

$$T_{He} = \left(\frac{1}{T} + \frac{\lambda_T}{2 \sum_i (F_i C_{p,i})} \right)^{-1} \quad (14)$$

Optimal control theory allows the use of either specified or free boundary conditions at the reactor inlet and the reactor outlet. This corresponds to the following eight necessary conditions for the boundaries

$$x_{n,0} = x_{n,0,specified} \quad \text{or} \quad \lambda_{n,0} = 0 \quad (15)$$

$$x_{n,L} = x_{n,L,specified} \quad \text{or} \quad \lambda_{n,L} = 0 \quad (16)$$

4. Calculations

The conservation eqs 2−5 and their corresponding inlet conditions form an initial value problem. This problem has been solved using the 'ode15s'-function of Matlab. For an optimized reactor, eq 5 is replaced by the helium temperature profile that is the outcome of the optimization scheme.

The combination of the eight differential equations given by 12 and 13, the single algebraic eq 14, and the eight boundary conditions given by 15 and 16 forms a two-point boundary value problem. This problem has been solved using the 'bvp4c'-function of Matlab. In addition to functions describing the differential equations and boundary conditions, the 'bvp4c'-function also requires a reasonable initial guess as input. This initial guess is obtained by performing one arbitrary constrained minimization. The quantity that is minimized is the total entropy production, and the conservation equations as well as the boundary conditions are used as constraints. The outcome of the complete optimization scheme is always a profile of the helium temperature along the reactor length. The helium temperature is in this case not constrained by a constant helium flow; we allow any temperature profile that minimizes the entropy production. All calculations have been done without experiencing numerical problems.

4.1. Input Data. A recent flow sheet of the sulfur−iodine process is used as basis for the reactor inlet and outlet conditions.[13] These conditions are listed in Table 1. Values for the physical parameters are based on various literature sources, which are listed in Table 2.

Table 1. Reactor Inlet and Outlet Conditions[13]

condition	value
inlet H_2O fraction (unitless)	0.481
inlet H_2SO_4 fraction (unitless)	0.094
inlet SO_3 fraction (unitless)	0.425
inlet temperature (K)	800
inlet pressure (bar)	7.09
outlet H_2O fraction (unitless)	0.458
outlet H_2SO_4 fraction (unitless)	0.001
outlet SO_3 fraction (unitless)	0.155
outlet SO_2 fraction (unitless)	0.257
outlet O_2 fraction (unitless)	0.129
helium inlet temperature (K)	1123
helium outlet temperature (K)	975

Table 2. Physical Parameters

parameter	value	reference
overall heat transfer coefficient ($J \cdot m^{-2} \cdot K^{-1} \cdot s^{-1}$)	170	15
helium heat capacity ($J \cdot mol^{-1} \cdot K^{-1}$)	20.8	16
gas viscosity ($kg \cdot m^{-1} \cdot s^{-1}$)	4.0×10^{-5}	16, 17
catalyst bed void fraction (unitless)	0.45	11
catalyst pellet density ($kg \cdot m^{-3}$)	4.2×10^{3}	17
catalyst pellet diameter (m)	3.0×10^{-3}	15
reactor diameter (m)	3.0×10^{-2}	15

All thermodynamic quantities like the enthalpies of reaction, Gibbs energies of reaction, component heat capacities, and equilibrium constants are calculated using tabulated values of thermodynamic coefficients.[16] The consistency of the data set can be verified using an entropy balance, where S_{in} represents the entropy in the inlet reaction mixture, S_{out} is the entropy in the outlet reaction mixture, and the remaining term is the entropy added due to heat transfer:

$$\frac{dS_{irr}}{dt} = S_{out} - S_{in} - \pi D \int_{z_0}^{L} \left(\frac{J'_q}{T_{He}} \right) dz \quad (17)$$

Equations 8 and 17 should yield the same total entropy production, which is indeed the case for the data used in this work. This means that the input data and model that we use in this study are consistent. Equation 17 also shows what the effect of minimizing the entropy production is: when the inlet, the outlet, and the total energy flow remain the same, a decrease in the entropy production must involve a decrease in the average helium temperature.

4.2. Three Reactor Designs. To compare the two approaches to reduce entropy production, three reactors are conceptually designed. The first design is based on conventional design rules and is used for comparison; it will be referred to as the reference reactor. The second design is the result of the functional optimization scheme and will be referred to as the optimized reactor. The third design is based on the elongation method and will be referred to as the elongated reactor.

The reference reactor is designed according to standard engineering practice. In parallel with similar reactor designs,[11,15] the reactor length was required to satisfy a reactor length-to-diameter ratio in the order of 100. A total initial molar flow rate of 0.034 $mol \cdot s^{-1}$ was selected, which corresponds to a sulfur dioxide production of 0.010 $mol \cdot s^{-1}$ and a reactor length of 2.17 m. The residence time of the reactor is 3.58 s and the pressure drop amounts 0.14 bar. The required helium flow rate amounts 0.588 $mol \cdot s^{-1}$.

The optimized reactor design is exactly the same as the reference reactor, except for its liberated helium temperature profile and its length. The length is not optimized in the strict

Table 3. Overview of the Most Important Fixed, Calculated, and Optimized Quantities That Are Used in the Three Reactor Models

quantity	reference reactor	optimized reactor	elongated reactor
F_0	fixed	fixed at reference value	fixed at reference value
$\xi_{1,0}$	fixed	fixed at reference value	fixed at reference value
$\xi_{2,0}$	fixed	fixed at reference value	fixed at reference value
p_0	fixed	fixed at reference value	fixed at reference value
T_0	fixed	fixed at reference value	fixed at reference value
$T_{He,0}$	fixed	optimized	calculated
$\xi_{1,L}$	calculated	optimized	calculated
$\xi_{2,L}$	fixed	fixed at reference value	fixed at reference value
p_L	calculated	fixed at reference value	calculated
T_L	calculated	optimized	calculated
$T_{He,L}$	fixed	optimized	fixed at reference value
$T_{He}(z)$	−	optimized	−
L	calculated	optimized	calculated
dS_{irr}/dt	calculated	optimized	fixed at optimum value

sense; the pressure drop is prescribed to equal that of the reference reactor and the reactor length has to change in order to realize this constraint. The influence of using free reactor outlet boundary conditions was also investigated. It turned out that the use of free boundary conditions for the temperature and the conversion of the first subreaction I yielded a lower entropy production without significantly changing the outlet values. Therefore, free outlet boundary conditions have been used for these two variables. The outlet boundary conditions of the pressure and the conversion of the second subreaction II remained fixed at their reference values. The optimal reactor length has been determined by performing the optimization scheme for a selected range of reactor lengths.

The elongated reactor is designed in such a way that it produces the same amount of entropy as the optimized reactor. This is realized by allowing an increased pressure drop, keeping in mind that a higher pressure drop will lead to an entropic penalty elsewhere in the process. Nonetheless, enforcing the same entropy production as in the optimized reactor facilitates the comparison between the two approaches. The helium inlet temperature and the conversion of the second subreaction are fixed at the values of the reference reactor. In addition to the reactor length also the helium flow rate and the total pressure drop are used as variables.

Table 3 gives an overview of the most important quantities that are used in the three reactor models. For each model it is shown whether these quantities are fixed at a certain value, the result of a normal calculation or the result of an optimization.

5. Results

5.1. The Reference Reactor. Figure 3 shows the profiles of the helium temperature T_{He}, the reaction mixture temperature T, the conversion of the sulfuric acid dissociation reaction ξ_1, the conversion of the sulfur trioxide decomposition reaction ξ_2, and the equilibrium conversion of the decomposition reaction $\xi_{2,eq}$. The equilibrium conversion is the conversion that would be attained at equilibrium, given the actual temperature. No equilibrium conversion for the dissociation reaction I is shown, because the dissociation conversion is modeled to equal the equilibrium conversion at all times.

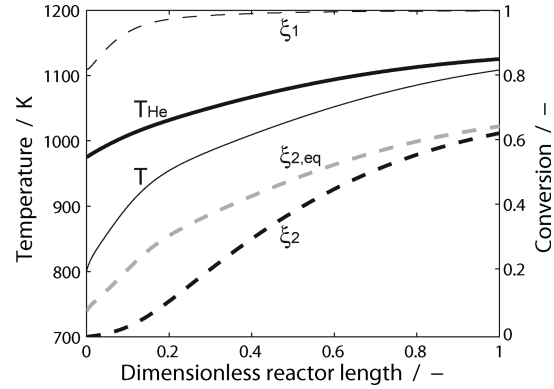

Figure 3. Reference reactor: temperature of the reactor T (normal line) and of the heating utility T_{He} (bold line) along the reactor length coordinate. Conversion of the sulfuric acid dissociation ξ_1 (normal dashed line) and of the sulfur trioxide decomposition ξ_2 (bold dashed line) along the reactor length coordinate. The equilibrium conversion $\xi_{2,eq}$ (gray bold dashed line) is shown for comparison.

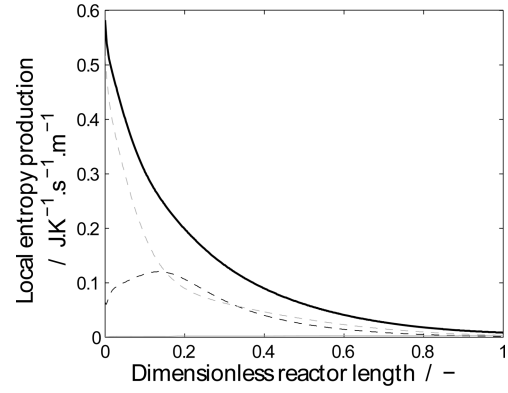

Figure 4. Reference reactor: Total entropy production σ_{tot} (bold line) as well as the three contributions due to heat transfer σ_q (gray dashed line), due to reactions σ_{rx} (dashed line), and due to frictional flow σ_{ff} (gray line, almost zero).

Following the dimensionless reactor length, the helium temperature profile increases smoothly from the reactor inlet to the reactor outlet. Since the helium is flowing countercurrently, this means that the helium temperature is decreasing from the helium inlet to the helium outlet. The mixture temperature shows a relatively steep increase near the inlet of the reactor, and levels off to a more flat increase. The difference between the two temperatures reduces constantly, and at the end of the reactor it is almost constant. The final temperature of the mixture is around 1108 K. The dissociation conversion I starts at its specified inlet value of 0.82 and after an initial steep increase at the reactor inlet, it slowly approaches completion. At the end of the reactor there is practically no sulfuric acid left. The decomposition conversion II increases slowly near the reactor inlet and outlet, most of the conversion takes place in the middle part of the reactor. The conversion at the outlet has the required value of 0.623. The difference between the actual and equilibrium conversions shows a maximum around 20% of the reactor length.

Figure 4 provides profiles for the total local entropy production σ_{tot} and its three components; the local entropy production due to heat transfer σ_q, chemical reactions σ_{rx}, and frictional flow σ_{ff}. The entropy production of the first subreaction is much smaller than the entropy production of the second subreaction, therefore the sum of both subreactions is shown.

It can immediately be seen that the frictional flow component is negligible compared to the other components; it is practically

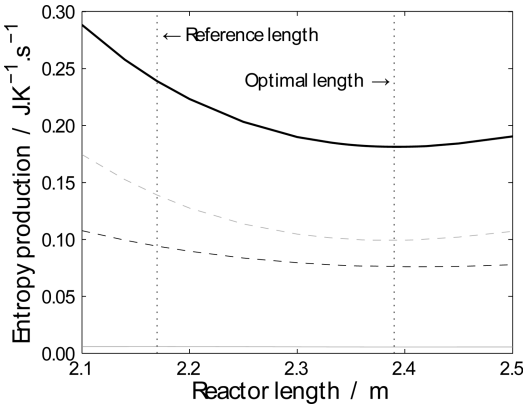

Figure 5. Variation of the entropy production with reactor length L for reactors with optimized helium temperature profile: the total entropy production (bold line) and the contributions due to heat transfer (gray dashed line), due to chemical reactions (dashed line), and due to frictional flow (gray line).

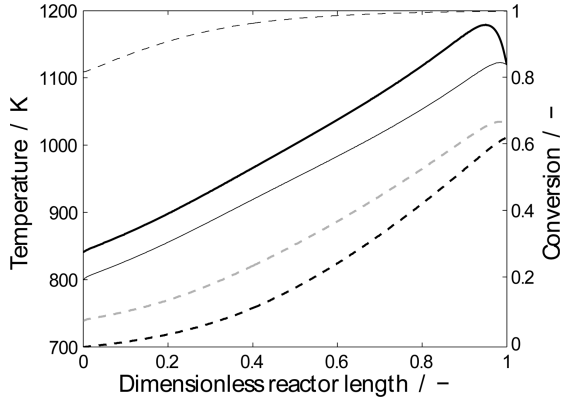

Figure 6. Optimized reactor: Temperature of the reactor T (normal line) and of the heating utility T_{He} (bold line) along the reactor length coordinate. Conversion of the sulfuric acid dissociation ξ_1 (normal dashed line) and of the sulfur trioxide decomposition ξ_2 (bold dashed line) along the reactor length coordinate. The equilibrium conversion $\xi_{2,eq}$ (gray bold dashed line) is shown for comparison.

invisible in the figure. The other two components are comparable in the largest part of the reactor. Only at the reactor inlet the heat transfer component dominates. It can be observed that almost all of the entropy is produced in the first third of the reactor, because the largest driving forces for entropy production can be found at the reactor inlet. However, only half of the final conversion is obtained in this first third of the reactor. The second half of the total sulfur dioxide conversion leads to a much lower entropy production compared to the first half. This difference in the amount of entropy produced per amount of sulfur dioxide converted suggests that improvements in the overall entropy production might be possible.

5.2. The Optimized Reactor. Figure 5 shows the total entropy production and its three separate components as a function of the length of the reactor. Both the heat transfer and reaction components have a considerable contribution to the total entropy production. The resulting minimum in the total entropy production corresponds to a reactor length of 2.39 m. The optimal reactor length and the length of the reference reactor are both indicated in Figure 5. The residence time of the reactor is 4.37 s.

Figure 6 shows the temperature and conversion profiles of the optimized reactor. The helium temperature profile increases linearly from a value of 841 K at the reactor inlet up to a maximum of 1179 K; next it decreases toward a value of 1119 K. The maximum temperature is well above the maximum reference temperature of 1125 K. The helium flow rate profile that corresponds to this helium temperature profile has an average of 0.256 mol·s^{-1}. The mixture temperature follows the same trend as the helium temperature. The resulting temperature difference increases slowly from the inlet of the reactor toward the end. At the end it shows a steep decrease and becomes zero at the outlet. This is the result of the free outlet boundary condition for the temperature, as can be seen when introducing the free outlet boundary condition $\lambda_{T,L} = 0$ into eq 16. The difference between the actual and equilibrium decomposition conversion shows a maximum around 50% of the reactor length.

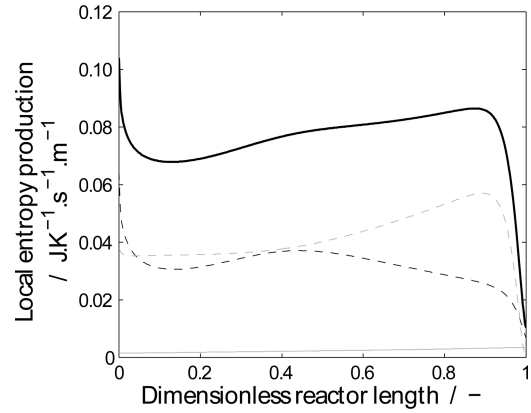

Figure 7. Optimized reactor: total entropy production σ_{tot} (bold line) as well as the three contributions due to heat transfer σ_q (gray dashed line), due to reactions σ_{rx} (dashed line), and due to frictional flow σ_{ff} (gray line).

Figure 7 shows the local entropy production profiles of the optimized reactor. At the inlet of the reactor the reaction component of the local entropy production is the most dominant one, but its contribution drops rapidly. In the middle of the reactor it remains relatively constant, and it drops again at the reactor outlet. Compared to the reference reactor the total entropy production is quite evenly distributed over the reactor length, except for the reactor inlet and outlet.

5.3. The Elongated Reactor. To obtain exactly the same outlet decomposition conversion, helium inlet temperature, and total entropy production, the elongated reactor requires a length of 2.91 m and a helium flow rate of 0.396 mol·s^{-1}. The residence time of the reactor is 4.90 s. Figure 8 shows the temperature and conversion profiles of the elongated reactor.

The trends in the temperature and conversion profiles of the elongated reactor are very similar to those of the reference reactor. The main changes are smaller differences between the helium and reaction mixture temperatures and between the actual and equilibrium decomposition conversions. The helium outlet temperature decreases to 902 K and the total pressure drop of the elongated reactor is 31% higher compared to the reference reactor.

Figure 9 gives the local entropy production profiles of the elongated reactor. The trends of the local entropy production profiles of the elongated reactor are similar to the reference reactor but with a lower maximum of the reaction component.

6. Discussion

6.1. Reactor Design Comparison. Table 4 shows a quantitative comparison between the lengths and the total entropy production and its components of the reference reactor, the optimized reactor, and the elongated reactor. Both the optimized and the elongated reactors produce 26% less entropy than the

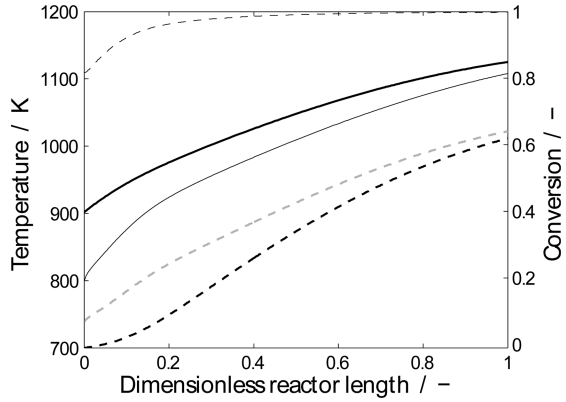

Figure 8. Elongated reactor: temperature of the reactor T (normal line) and of the heating utility T_{He} (bold line) along the reactor length coordinate. Conversion of the sulfuric acid dissociation ξ_1 (normal dashed line) and of the sulfur trioxide decomposition ξ_2 (bold dashed line) along the reactor length coordinate. The equilibrium conversion $\xi_{2,eq}$ (gray bold dashed line) is shown for comparison.

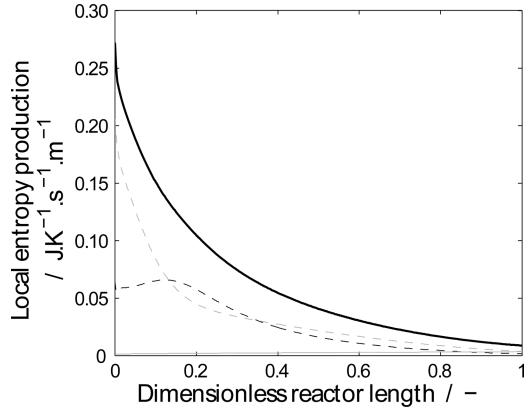

Figure 9. Elongated reactor: total entropy production σ_{tot} (bold line) as well as the three contributions due to heat transfer σ_q (gray dashed line), due to reactions σ_{rx} (dashed line), and due to frictional flow σ_{ff} (gray line).

Table 4. Quantitative Reactor Comparison

reactor design	reference	optimized	elongated
L (m)	2.17	2.39	2.91
σ_{rx} (J·K^{-1}·s^{-1})	0.094	0.076	0.075
σ_{q} (J·K^{-1}·s^{-1})	0.147	0.099	0.099
σ_{ff} (J·K^{-1}·s^{-1})	0.006	0.006	0.008
σ_{tot} (J·K^{-1}·s^{-1})	0.246	0.181	0.181

reference reactor. As explained in section 4.2, the elongated reactor was required to have the same reduction as the optimized reactor. The reductions in entropy production are in both cases caused by the reaction and heat transfer components. The frictional flow component of the elongated reactor even increases, this is mainly related to the increased reactor length.

Figure 10 shows a comparison between the distributions of the total entropy production over the dimensionless reactor length of the reference reactor, the optimized reactor, and the elongated reactor. It can be seen that the optimization method indeed yields a more evenly distributed total entropy production profile. A small maximum still exists at the reactor inlet however; it is caused by the chemical reactions and related to the fixed inlet conditions. Two important concepts in the work of Johannessen and Kjelstrup are the equipartition of entropy production (EoEP) and the equipartition of forces (EoF). A hypothesis is proposed stating that "EoEP, but also EoF are good approximations to the state of minimum entropy production in the parts of an optimally controlled system that have sufficient freedom."[18] If we look at the optimized reactor results, we can see that they correspond very well with the hypothesis. The optimal profile approximates EoEP in the middle part and the fixed boundary conditions cause the peaks in entropy production at the inlet and outlet.

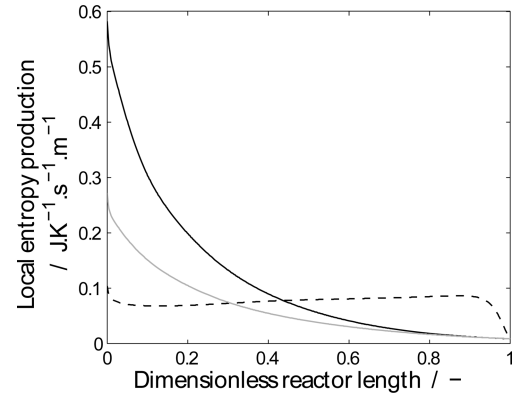

Figure 10. Comparison of the total local entropy production σ_{tot} along the reactor length coordinate for the reference reactor (normal line), the optimized reactor (dashed line), and the elongated reactor (gray line).

The effect of the elongation method on the total entropy production profile can be seen when comparing the reference reactor with the elongated reactor. The trends of the profiles remain the same, but the absolute values change.

6.2. Comparing the Two Methods. Both the optimized and the elongated reactors produce 26% less entropy, but the way in which this reduction is obtained is different. The optimized reactor is optimized in reactor length and a variable helium flow rate is allowed. The variable helium flow requires that helium is added and removed along the reactor length. The maximum in helium temperature is higher than in the other designs. Because this maximum is no longer positioned at the reactor outlet, the helium flow direction becomes cocurrent in the last part of the reactor. The helium outlet temperature (at the reactor inlet) decreases from 975 to 841 K, with a decrease in the average helium flow rate from 0.588 to 0.256 mol·s^{-1} as a result. The elongated reactor has a helium temperature at the reactor inlet of 902 K, with a corresponding helium flow rate of 0.396 mol·s^{-1}. It requires a 34% longer reactor; the residence time in the reactor is increased by 37%, and in addition an increase in the pressure drop of 31% is introduced. To compensate for this increased pressure drop, additional compressor duty is required, which results in an increase in the entropy production. So a part of the achieved reductions in entropy production of the reactor is countered by an increase elsewhere in the process, in addition to the increased material costs of the reactor.

In general it can be concluded that the optimized reactor requires a substantially smaller increase in reactor length than the elongated reactor. The helium flow rate of the optimized reactor is lower and the reduction in entropy production that is achieved is a permanent improvement; it is not countered by an increase in the entropy production elsewhere in the process. However, it is demanding to realize the appropriate heating equipment in a practical design.

7. Conclusions

This work has shown that considerable improvements are possible in the exergy efficiency of thermochemical hydrogen production from water. The sulfuric acid decomposition step

of the sulfur−iodine process has been studied in particular. Starting from a reference decomposition reactor, two reactors have been conceptually designed that both produce 26% less entropy; an optimized reactor and an elongated reactor.

The optimized reactor uses a variable helium flow rate instead of a constant one and is optimized in length. It is characterized by a more even distribution of the entropy production over the entire reactor length, which corresponds to equipartition of entropy production. The outlet helium temperature from the endothermic reactor drops from 975 to 841 K and the average helium flow rate is 56% lower than the constant helium flow rate of the reference reactor.

The elongated reactor is 34% longer than the reference reactor but a 31% higher pressure drop is allowed. The need for extra compressor duty to compensate for the increased pressure drop results in an increased entropy production elsewhere in the process. The entropy production in the reactor is pronounced at the reactor inlet, similar to the reference reactor. The helium outlet temperature drops from 975 to 902 K and the helium flow rate is decreased by 33%.

Overall, the optimization method yields a thermodynamically better reactor design than the elongation method, but it requires significant changes to the heating equipment. In general, it can be concluded that a lower helium temperature at the reactor inlet should be used. The practical gain of the achieved reduction in entropy production is that a part of the high temperature heat input is replaced with heat of a lower temperature. Information on the exact temperature can only be obtained from a Second Law analysis.

Acknowledgment

The authors thank Eivind Johannessen for providing a Matlab implementation of the algorithm that served as a basis for our study.

Supporting Information Available: Rate constants of sulfuric acid decomposition. This material is available free of charge via the Internet at http://pubs.acs.org.

Literature Cited

(1) Funk, J. E. Thermochemical hydrogen production: past and present. *Int. J. Hydrogen Energy* **2001**, *26*, 185.

(2) Lior, N.; Zhang, N. Energy, exergy and Second Law performance criteria. *Energy* **2007**, *32*, 281.

(3) Kotas, T. J. *The Exergy Method of Thermal Plant Analysis*; Butterworths: London, 1985.

(4) Leites, I. L.; Sama, D. A.; Lior, N. The theory and practice of energy saving in the chemical industry: some methods for reducing thermodynamic irreversibility in chemical technology processes. *Energy* **2003**, *28*, 55.

(5) Rosen, M. A.; Scott, D. S. Entropy production and exergy destruction: Part II—illustrative technologies. *Int. J. Hydrogen Energy* **2003**, *28*, 1315.

(6) Bejan, A.; Tsatsaronis, G.; Moran, M. *Thermal Design and Optimization*; Wiley: New York, 1996.

(7) Kjelstrup, S.; Bedeaux, D.; Johannessen, E. *Elements of Irreversible Thermodynamics for Engineers*; Tapir Academic Press: Trondheim, Norway, 2006.

(8) Tondeur, D.; Kvaalen, E. Equipartition of entropy production. An optimality criterion for transfer and separation processes. *Ind. Eng. Chem. Res.* **1987**, *26*, 50.

(9) Kjelstrup Ratkje, S.; Sauar, E.; Hansen, E. M.; Lien, K. M.; Hafskjold, B. Analysis of entropy production rates for design of distillation columns. *Ind. Eng. Chem. Res.* **1995**, *34*, 3001.

(10) Sauar, E.; Kjelstrup Ratkje, S.; Lien, K. M. Equipartition of Forces: A new principle for process design and optimization. *Ind. Eng. Chem. Res.* **1996**, *35*, 4147.

(11) Johannessen, E.; Kjelstrup, S. Minimum entropy production in plug flow reactors: An optimal control problem solved for SO_2 oxidation. *Energy* **2004**, *29*, 2403.

(12) Ginosar, D. M.; Petkovic, L. M.; Glenn, A. W.; Burch, K. C. Stability of supported platinum sulfuric acid decomposition catalysts for use in thermochemical water splitting cycles. *Int. J. Hydrogen Energy* **2007**, *32*, 482.

(13) Brown, L. C.; Besenbruch, G. E.; Lentsch, R. D.; Schlutz, K. R.; Funk, J. E.; Pickard, P. S.; Marshall, A. C.; Showalter, S. K. *High Efficiency Generation of Hydrogen Fuels Using Nuclear Power*; General Atomics Report GA-A24285, 2003.

(14) de Groot, S. R.; Mazur, P. *Non-equilibrium Thermodynamics*; North-Holland Publishing Company: Amsterdam, The Netherlands, 1962.

(15) Lin, S. S.; Flaherty, R. Design studies of the sulfur trioxide decomposition reactor for the sulfur cycle hydrogen production process. *Int. J. Hydrogen Energy* **1983**, *8*, 589.

(16) NIST Chemistry WebBook, NIST Standard Reference Database Number 69, June 2005, http://webbook.nist.gov/chemistry/. (Accessed Dec 2007).

(17) *CRC Handbook of Chemistry and Physics*; CRC Press, Boca Raton, FL, 1995.

(18) Johannessen, E.; Kjelstrup, S. A highway in state space for reactors with minimum entropy production. *Chem. Eng. Sci.* **2005**, *60*, 3347.

Received for review October 22, 2008
Revised manuscript received March 20, 2009
Accepted July 2, 2009

IE801585E